Programmable Chirp Compensation for 6-fs Pulse Generation with a Prism-Pair-Formed Pulse Shaper

Lin Xu, *Member, IEEE,* N. Nakagawa, R. Morita, H. Shigekawa, and M. Yamashita

***Abstract*—We describe a TF5 prism-pair-formed pulse shaper for programmable pulse chirp compensation. The advantages of this kind of pulse shaper are: 1) very broad bandwidth of transmission; 2) smaller losses; and 3) no requirement for a large-size spatial light modulator (SLM) if the input spectrum is very broad. In our experiment, an ultrabroad spectral (500–1000 nm) pulse is produced by launching 1-kHz, 30-fs, 400-μJ pulses at 780 nm into an argon-filled glass capillary fiber at the gas pressure of 2.0 bar. The fiber has an inner diameter of 140 μm and a length of 60 cm. The chirped pulse is first precompressed by a pair of BK7 prisms with a separation length of 65 cm and then directed into the prism-pair-formed pulse-shaping apparatus with a 128-pixel SLM, which provides quadratic and cubic phase compensation. When the quadratic and cubic phases are -330 fs^2 and $+2000$ fs^3, respectively, at the wavelength of 760 nm, an ultrashort optical pulse of 6 fs (FWHM) is generated. This is, to the best of our knowledge, the shortest optical pulse ever compressed using the SLM pulse-shaping technique.**

***Index Terms*—Nonlinear-chirp compensation, prism pair, programmable pulse shaping, pulse compression, spatial light modulator (SLM), ultrabroad spectrum, ultrashort pulse.**

I. Introduction

THE RECENT development of ultrashort optical-pulse technology has enabled us not only to clarify transient processes in the sub-10-fs time region in physics, chemistry, and biology but also to produce new information technology such as high-speed optical communications and optical computing [1]. These novel fields drive us to further develop optical sources for generating shorter and shorter pulses. The fundamental limit on the shortness of the temporal duration of an ultrashort pulse is determined by the uncertainty relation ($\Delta\nu\Delta t = k$, $\Delta\nu$, Δt and k are the spectral width, the pulse duration, and a constant relating to the pulse shape, respectively). This shows that the first condition for obtaining a short pulse is to produce a broad bandwidth. This can be achieved by seeking a gain medium with a broader fluorescence emission for a laser oscillator (such as Ti : sapphire [2]) or by broadening a pulse spectrum extracavity by self-phase modulation (SPM) [3], [4] or induced-phase modulation [5]–[8]. The second condition for short pulse generation concerns pulse chirp compensation since different wavelengths of a short pulse travel at different speeds through any material, resulting in a broadened and chirped pulse. This becomes even more important with shorter pulses, as the dispersion has to be compensated for over a large spectral range. Consequently, improvements in pulse compression or dispersion-compensation techniques advance the progress of ultrashort pulse generation.

Prism-pair or grating-pair compressors are commonly used for second-order dispersion compensation, and a combination of these compressors allows us to compensate for third-order dispersion and, consequently, to generate 6-fs pulses in a dye laser system [9]. Recently, chirped mirrors [10], [11] and double-chirped mirrors [12], [13] were tailored to produce negative group-velocity dispersion (GVD) over a wide spectrum. The combinations with the prism-pair or grating-pair generated pulses with a duration of 4–5-fs by external pulse compression [14]–[16], from an optical parametric amplifier [17] and directly from Ti : sapphire oscillators [18], [19]. However, these methods have drawbacks concerning the interdependence among different dispersion orders, which prevent perfect high-order dispersion compensation, and limited-transmission bandwidth due to chirped mirrors [10]–[13]. A kind of so-called active pulse compression technique, which utilizes an active phase-control element as a variable phase mask in zero-dispersion pulse shaping, can realize independently different orders of phase control. This has been demonstrated by use of liquid crystal spatial light modulators (SLM's) [20], [21] acoustooptic modulators [22] and mechanically deformable mirrors [23]. Among them, programmable pulse shaping by using a SLM as a phase mask can impart large cubic and higher order phases to a transform-limited femtosecond pulse, and hence manifests the capability of arbitrary phase control to generate a monocycle optical pulse [5], [6], [20], [21]. Yelin *et al.* experimentally demonstrated the first adaptive femtosecond pulse compression [24]. The compressor was operated with a programmable 128-pixel commercial SLM which was addressed by a feedback-controlled self-learning algorithm, resulting in automated phase compensation. As a result, an 80-fs strongly chirped pulse was compressed to 11 fs at 800 nm. This technique was also applied in Ti : sapphire amplifier systems [25], [26] and fiber communication applications [27] for high-order-dispersion compensation.

In this paper, we present a prism-pair-formed pulse shaper with a programmable SLM for chirp-compensation. The optimization of chirp-compensation results in the generation of 6-fs optical pulses. This is, to the best of our knowledge, the shortest

Manuscript received December 6, 1999; revised May 1, 2000.

L. Xu was with the Department of Applied Physics, Hokkaido University, Sapporo 060-8628, Japan, and CREST, Japan Science and Technology Corporation. He is now with the School of Physics, Georgia Institute of Technology, Atlanta, GA 30332 USA.

N. Nakagawa, R. Morita, and M. Yamashita are with the Department of Applied Physics, Hokkaido University, Sapporo 060-8628, Japan, and CREST, Japan Science and Technology Corporation. Saitama Pref. 332-0012, Japan.

H. Shigekawa is with the Institute of Materials Science, University of Tsukuba, Tsukuba 305-8573, Japan and CREST, Japan Science and Technology Corporation.

Publisher Item Identifier S 0018-9197(00)06167-4.

pulse ever compressed by the SLM pulse-shaping technique. In our experiment, the gratings employed conventionally are replaced by highlydispersive Brewster-angle cut TF5 prisms. The advantages of the prism-pair-formed pulse shaper compared with its grating-pair counterpart lie in: 1) a broad bandwidth of high transmission; 2) the requirement of a small-size SLM when the input pulse spectrum is very broad; and 3) better linear frequency distribution as a function of spatial position, which benefits programmable chirp-compensation.

II. Prism-Pair-Formed Pulse Shaper for Phase Compensation

A. Prism-Pair-Formed Pulse Shaper

In a pulse shaper, the pulse to be shaped is spatially dispersed using an angular dispersive element. The dispersed frequency components are collimated and focused by a lens or a spherical mirror onto the different spots at the Fourier plane where a liquid crystal phase modulator is located. The second lens or mirror and the angular dispersive element recombine each of the separate frequency components into a single output beam. Typically, the diffraction gratings are the angular elements and the formed-4-f pulse shaper is a dispersion-free system. The angular dispersion of a grating is usually defined as the rate of change of angle with a change in wavelength: $\delta\theta_d/\delta\lambda = m/d\cos(\theta_d)$. Here, θ_d represents the diffraction angle, m represents the diffraction order, and d is the grating period. The relation shows that the larger the grating period is, the less widely the spectra are spread. This may become important when a shorter pulse is shaped because the shorter pulse corresponds to the broad spectral bandwidth in the frequency domain. In this case, coarse gratings (a large grating period) are usually utilized to match the size of a commercially available SLM (128 pixels with an aperture around 13 mm). On the other hand, the diffraction efficiency bandwidth of the grating diminishes as the grating period increases (the coarse grating). This definitely yields problems for pulses with durations approaching a few femtoseconds. Fortunately, these problems can be solved for prisms cut at the Brewster angle due to their smaller angular dispersion and their large high-transmission bandwidth as compared with gratings. Furthermore, the linearity of the frequency distribution of a prism as a function of the spatial position at the focal plane is better than that of a grating. This benefits programmable chirp-compensation. A drawback of the prism-pair-formed 4-f pulse shaper is that it is not free of dispersion because of the material dispersion of prisms. However, the dispersion can be removed by another prism pair.

The schematic of the prism-pair formed 4-f pulse shaping system is shown in Fig. 1(a). It consists of a pair of highly dispersive TF5 prisms cut at Brewster's angle at 780 nm, P1 and P2, and a pair of concave 200-mm focal-length spherical mirrors, M1 and M2. The programmable one-dimensional (1-D) 128-pixel liquid crystal SLM (Meadowlark Optics, SLM2256) is placed at the Fourier plane of the shaper where frequencies are spatially dispersed. The width of each pixel is 97 μm, and the inter-pixel gap is 3 μm. In order to realize programmable phase control of the SLM, we evaluate the frequency distribution on

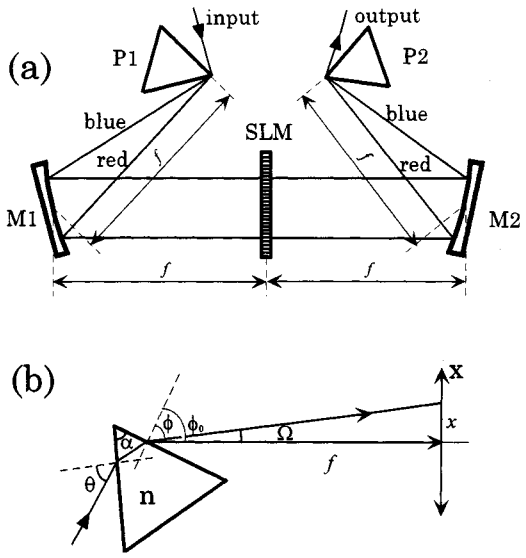

Fig. 1. (a) Schematic of a prism-pair formed 4-f pulse shaper. A pulse is spatially dispersed by a prism P1 and then collimated and focused by a spherical mirror M1 onto a liquid-crystal phase modulator which is located at the Fourier plane of a $4-f$ system. The output beam is recombined by a second mirror M2 and prism P2. (b) Geometry for calculating the spatial distribution of a Brewster prism in the Fourier plane. θ represents the incident angle to the prism, $\phi(\lambda)$ is the refractive angle of the wavelength λ, and ϕ_0 is the refractive angle at the center wavelength λ_0.

the SLM plane. The geometry for the calculation of spatial dispersion in the masking plane is shown in Fig. 1(b). Let θ be the angle of incidence on the prism, and $\phi(\lambda)$ the refractive angle at the wavelength λ. The angle $\phi(\lambda)$ can be derived to be [28]:

$$\phi(\lambda) = \arcsin\Big[\sin(\theta)\cos(\pi-\alpha) + \sin(\pi-\alpha)\sqrt{n(\lambda)^2-(\sin(\theta))^2}\Big] \quad (1)$$

where α is the apex angle of the prism and $n(\lambda)$ represents the refractive index of the prism. For the TF5 prism, the refractive index n is 1.738 at 780 nm [29], and the Brewster angle is evaluated as 60 deg; thus, $\theta = 60$ deg, and $\alpha = 60$ deg. If the distance between the prism and the masking plane is set to f, and $\Omega = \phi_0 - \phi$, where ϕ_0 is the refractive angle of the center wavelength λ_0, the position x of the wavelength λ in the masking plane is given by

$$x = f\tan\Omega. \quad (2)$$

To evaluate the spatial position, we expand the position $x(\lambda)$ in the masking plane with respect to λ in a Taylor series

$$x(\lambda) = x_0 + x^{(1)}(\lambda_0)(\lambda-\lambda_0) + \frac{1}{2!}x^{(2)}(\lambda_0)(\lambda-\lambda_0)^2 + \cdots + \frac{1}{n!}x^{(n)}(\lambda_0)(\lambda-\lambda_0)^n + \cdots \quad (3)$$

where $x^{(n)}(\lambda_0)=(d^n x/d\lambda^n)|_{\lambda=\lambda_0}$, λ_0 is the center wavelength of the pulse, and x_0 is the position of the center wavelength $(x_0 = 0)$. From (1) and (2), the derivatives of $x^{(n)}(\lambda_0)$ can be numerically evaluated, and, using (3), we calculate the wavelength and angular-frequency distributions at the SLM plane as

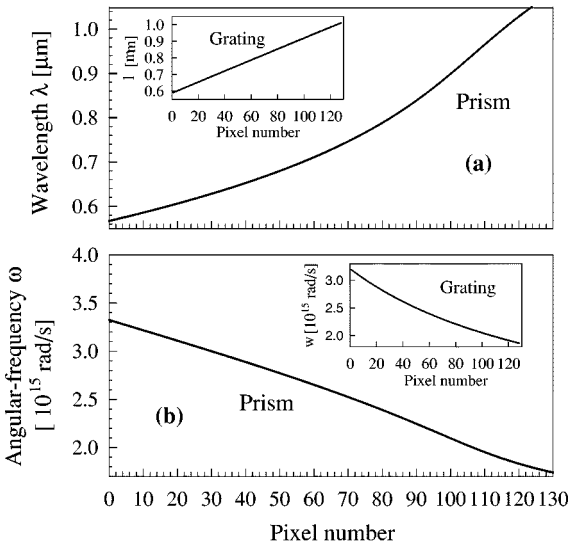

Fig. 2. (a) Spatial wavelength dispersion and (b) spatial angular-frequency dispersion at the Fourier plane of the TF5 prism-pair-formed pulse shaper. The spatial dispersion features of a grating partner are shown in the insets (here, $d = 1/300$ mm, $f = 100$ mm, and $\phi(\lambda_0) = 6.9$ deg).

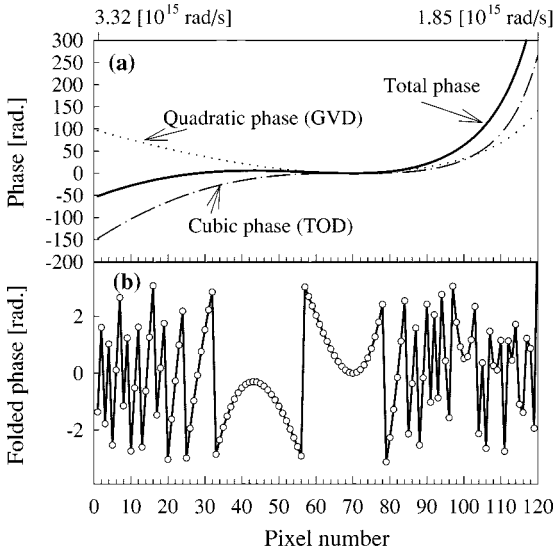

Fig. 3. (a) The phases imparted on the SLM in the TF5 prism-formed pulse shaper when $d^2\phi/d\omega^2|_{\omega_0} = -330$ fs^2 and $d^3\phi/d\omega^3|_{\omega_0} = +2000$ fs^3 ($\lambda_0 = 760$ nm). (b) The folded phases within $[-\pi, \pi]$.

functions of the pixel number of the SLM to the third order in the Taylor series, which allows us to approach the real distributions. Here $f = 200$ mm. The results are shown in Fig. 2(a) and (b), respectively. The acceptable wavelength range is from 570 to 1070 nm for our 128-pixel SLM. Although the wavelength distribution is not linear, the angular-frequency distribution is almost linear over the range of 1.5×10^{15} rad/s (corresponding to 500 nm). To compare the spatial dispersion features of these two kinds of pulse shapers, the wavelength and angular-frequency distributions of the gratings are also evaluated at $d = 1/300$ mm, $f = 100$ mm, and $\phi(\lambda_0) = 6.9$ deg. The results are shown in the insets of Fig. 2. It shows that the linearity of the angular-frequency distribution of the prism is better than that of the grating when they both have the same acceptable angular-frequency range. It should be noted that the linear angular-frequency distribution benefits programmable phase control of the SLM because we will expand the phase applied to the SLM in a Taylor series with respect to the angular frequency, and the linear distribution means that a constant angular-frequency difference ($\Delta\omega$) exists between the adjacent pixels. This point will be discussed in Section II-B.

B. Phase Control by the SLM Within the Pulse Shaper

We have calibrated the angular-frequency distribution versus pixel number of the SLM (Fig. 2). For phase control of chirped pulses, we include the quadratic and cubic dispersion terms on the SLM as

$$\phi_{\mathrm{SLM}}(\omega_j) = \frac{1}{2!}\frac{d^2\phi}{d\omega^2}\bigg|_{\omega_0}(\omega_j-\omega_0)^2 + \frac{1}{3!}\frac{d^3\phi}{d\omega^3}\bigg|_{\omega_0} \cdot(\omega_j-\omega_0)^3+\cdots \tag{4}$$

where $j = 1, 2, \cdots, 128$ (pixel number). In practice, the center angular frequency ω_0 (corresponding to $\lambda_0 = 760$ nm) is set to $\omega_0 = \omega_{70}$, thus $\omega_j - \omega_0$ represents the angular-frequency difference between the jth pixel and the 70th pixel. If we have a perfect linear angular-frequency distribution on the SLM, $\omega_j - \omega_0$ will be $(j-70)\Delta\omega$ (where $\Delta\omega$ is the angular-frequency difference between arbitrary adjacent pixels). However, a nonlinear angular-frequency distribution will result in a large or small $\Delta\omega$ at both edges of the SLM. This nonlinear distribution effect may affect pulse shaping or pulse compression to the monocycle pulse duration level if the programmable control is operated (see Section IV).

When we set $d^2\phi/d\omega^2|_{\omega_0} = -330$ fs^2 and $d^3\phi/d\omega^3|_{\omega_0} = +2000$ fs^3 (at $\lambda_0 = 760$ nm), respectively, the phases on the SLM are evaluated to be as shown in Fig. 3(a). The dotted and dot–dashed lines depict the pure quadratic (GVD) and cubic [third-order dispersion (TOD)] phases, respectively. The solid line shows the total phase which is applied to the SLM. Since the components of the electric field spectrum of a short pulse are spectrally expanded on the SLM, chirp compensation by the programmable SLM is carried out in the frequency domain. The electric field in the frequency domain can be written as [30]: $E(\omega) = |E(\omega)|\exp(i\phi(\omega)) \equiv |E(\omega)|\exp[i(\Delta\phi(\omega)+m\cdot2\pi)]$. Here, $\Delta\phi(\omega)$ is within $[-\pi, \pi]$ and $m = 0, \pm1, \pm2, \cdots$. As a result, we can fold a larger phase $\phi(\omega)$ into $\Delta\phi(\omega) \in [-\pi, \pi]$, which is shown in Fig. 3(b). It should be noted that, in the case of chirp compensation, we do not need to adjust $\phi(\omega_0)$ (the absolute phase) and $\dot{\phi}(\omega_0)$ (the group delay) unlike the case of phase compensation of the CW wave, and, hence, $\phi(\omega)$ does not include these terms as given by (4). In order to accomplish phase control, it is necessary to calibrate the phase response of the SLM as a function of the applied voltage. This is done by using a He–Ne laser according to the method of [18] and a maximum phase shift in excess of 6π was measured. As our input pulse spectrum is very broad, calibrations for all wavelengths are needed. In [21], however, they found a uniformity of the phase shift in the range of 0–2π for all wavelengths studied (see [21, Fig. 2]). Accordingly, we employ this feature and calibrate our SLM in this range. Consequently, we are able to con-

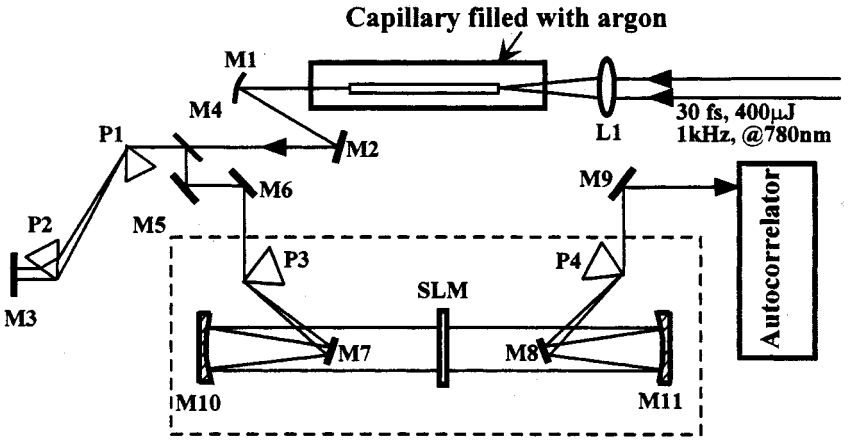

Fig. 4. Layout of experimental setup. M2–M9: silver-coated plane mirrors; M1, M10, and M11: Al-coated spherical mirrors; $R = -400$ mm; L1: $f = 300$ mm; P1, P2: Brewster-angle cut BK7 prisms; P3, P4: Brewster-angle cut TF5 prisms. The pulse shaper is shown within the dashed frame.

trol the voltages which are applied to the SLM to accomplish folded-phase-control over the entire wavelength range.

III. Experimental Setup and Results

A. Ultrabroad Spectrum Generation

As we discussed, there are two conditions for ultrashort pulse generation. The first condition is to generate a broad-bandwidth pulse. It can be realized by self-phase modulation (SPM) in a hollow fiber [14], [16]. Our experimental setup is shown in Fig. 4. We carry out the experiment using a multipass Ti : sapphire amplifier at a repetition rate of 1 kHz (FemtoPower PRO, FEMTO LASERS). The output pulses have a duration of 30 fs, energy up to 800 μJ, and a spectrum centered at 780 nm. A pulse of energy of 400 μJ is launched into an argon-filled glass capillary fiber with an inner diameter of 140 μm and a length of 60 cm. The fiber is placed in a high-pressure chamber with 1-mm-thick sapphire windows. At a gas pressure of 2.0 bar, the spectrum is broadened due to the dispersive SPM effect. The output pulse energy is around 42 μJ, corresponding to 10% coupling efficiency. This somewhat lower efficiency may be partly attributed to the uncoated AR-coating of the sapphire windows and partly to bending and surface-roughness losses. The measured spectrum, having a range from 500 to 1000 nm, is depicted in Fig. 5. The output pulse is strongly chirped with a duration of 177 fs full-width at half-maximum (FWHM) when measured with an intensity autocorrelator (inset of Fig. 5). The asymmetric autocorrelation trace is due to the noise introduced by the transmission of the fundamental signal since the short wavelength of the fundamental is just at the edge of the transmission bandwidth of the SHG filter which is placed in front of the autocorrelator detector. This has been verified by measuring the autocorrelation of a pulse with a slightly narrower specturm, in which case a perfectly symmetrical trace is observed.

B. A BK7 Prism-Pair for the Precompressor

The self-phase-modulated chirped pulse is collimated by a spherical mirror M1 with a focal length of 200 mm and then

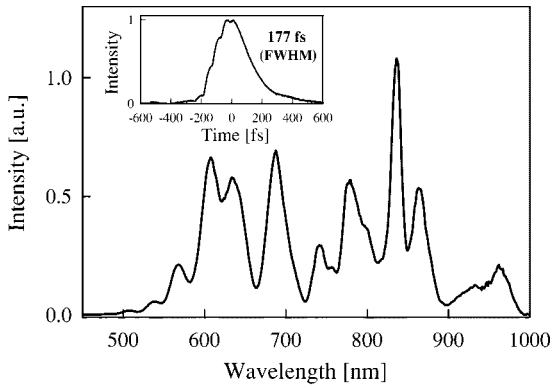

Fig. 5. The spectrum generated from an Ar-filled capillary fiber pumped by a 1-kHz, 30-fs, 400-μJ pulse centered at 780 nm. Inset: the intensity autocorrelation trace of the fiber-output chirped pulse with a duration of 177 fs (FWHM).

directed to a precompressor which consists of a pair of BK7 prisms cut at Brewster's angle at 780 nm (see Fig. 4). The precompressor is designed to compensate for material dispersions of the TF5 prism pair and the SLM in pulse shaping. The GVD and TOD of TF5 glass, SLM, BK7 glass, and a pair of BK7 prisms [29], [31] at 780 nm are shown in Table I. Assuming the optical paths within the TF5 prisms and the BK7 prisms are 4 and 24 mm (double passes), respectively, the BK7 prism pair with a separation length of 65 cm introduces a net GVD $=-80$ fs^2 and TOD $=-1645$ fs^3 when a pulse passes through the precompressor and the pulse shaper.

C. Chirp Compensation with SLM

The output from the precompressor is coupled into the pulse-shaping apparatus which is similar to Fig. 1. In order to reduce imaging distortion by astigmatic aberrations, two plane mirrors M7 and M8 are used to fold the beams (see Fig. 4). Therefore, the folding angles of the two spherical mirrors are kept as small as possible to alleviate aberrations. Two TF5 prisms are placed at the focal planes of a pair of concave spherical mirrors of the 200-mm focal length to form a 4-f system. The output pulse is directed to an interferometric autocorrelator with a 40-μm-thick

TABLE I
THE DISPERSION OF THE GLASS MATERIAL, SLM, AND A PRISM PAIR AT 780 nm

	GVD (fs^2)	TOD (fs^3)
TF5 glass (4 mm)[a]	+739	+257
SLM substrate (FS, 2mm)	+75	+54
BK7 glass (24 mm)	+1116	+754
BK7 prism-pair (separation length of 65 cm, double passes)	-2010	-2710
Total dispersion	-80	-1645

[a] Dispersion formula: $n(\lambda)^2 = A_1 + A_2\lambda^2 + A_3/\lambda^2 + A_4/\lambda^4 + A_5/\lambda^6 + A_6/\lambda^8$ for TF5 glass, $A_1 = 2.9580175$, $A_2 = -8.2686725*10^{-3}$, $A_3 = 39.383391 * 10^{-3}$, $A_4 = 12.219807 * 10^{-4}$, $A_5 = 3.1433368 * 10^{-5}$, $A_6 = 86.507903 * 10^{-7}$ [29].

BBO crystal (Femtometer, FEMTO LASERS) to monitor the compressed pulse duration. Since the net negative GVD from the precompressor is not sufficient for compensating for the linear part of the self-phase-modulated chirp, we first apply a negative quadratic phase (GVD) on the SLM. The increasing signals of autocorrelation are observed, corresponding to pulse shortening. When the quadratic phase at 760 nm imparted is -330 fs^2, the fringe-resolved autocorrelation (FRAC) is shown in Fig. 6(a). The incorrect rate of the peak to background hints that the nonlinear chirp is not compensated for [32]. When the *positive* cubic phase is added on the SLM, we observe that the FRAC becomes better and shorter. This means that the uncompensated pulse has residual *negative* cubic phase dispersion, which is mainly due to the large net negative TOD dispersion introduced by the precompressor and other optical elements (see Table I) but not due to the nonlinear chirp from the dispersive SPM. While the cubic phase is set to be $+1000$ fs^3, the better FRAC as shown in Fig. 6(b) is observed. The shortest optical pulses are generated when the cubic phase is $+2000$ fs^3 [its phase on the SLM is shown in Fig. 3(a)]. The FRAC is depicted in Fig. 6(c). From the fitting, assuming a sech^2(t) intensity profile, we obtain a pulse duration of 6 fs (FWHM) (solid line). The direct inverse Fourier transform of the compressed-pulse spectrum (Fig. 7) results in a 5.6 fs (FWHM) pulse (circles). The result gives good agreement with the measured FRAC indicating that the small residual phase error exists and the nonlinear chirp is almost compensated for. Fig. 7 shows the compressed-pulse spectrum, while the inset depicts the intensity profile of the inverse Fourier transform of the measured spectrum.

In order to compare the difference between the present compressor (the pulse shaper plus the pre compressor) and a general prism-pair compressor, we direct the output pulse from the precompressor to the autocorrelator. With more of the second BK7 prism inserted (to balance the large negative GVD designed for compensating for material dispersion of the TF5 prisms and the SLM), a shorter pulse is produced. However, the larger structures on the wings of the FRAC are observed, as shown in Fig. 8,

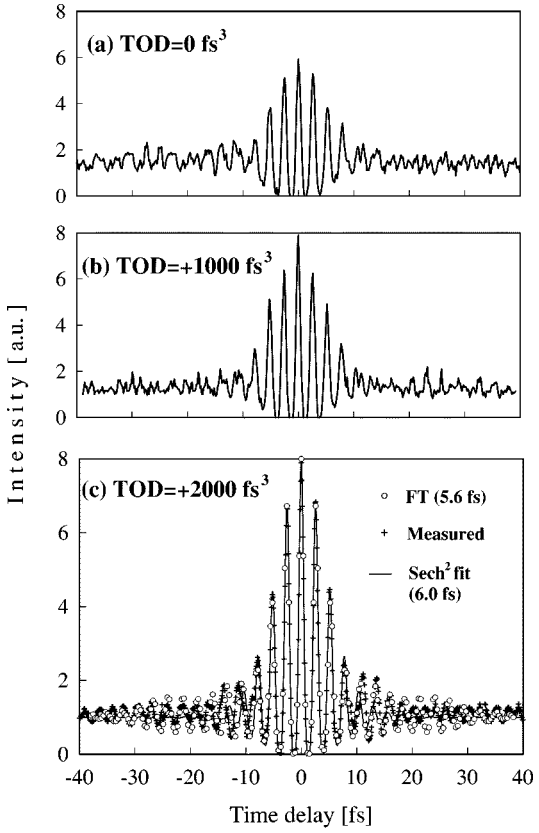

Fig. 6. The measured FRAC's when applied phases of GVD $=-330$ fs^2 and: (a) TOD $=0$ fs^3, (b) TOD $=+1000$ fs^3, and (c) TOD $=+2000$ fs^3. On curve (c), the fitting of a sech^2 gives a 6-fs pulse (FWHM) (solid line), and the calculation from the inverse Fourier transform of the measured pulse spectrum is 5.6 fs (FWHM) (circles).

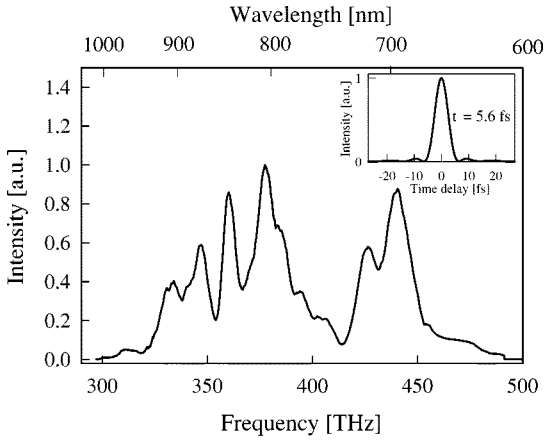

Fig. 7. The measured spectrum of the shortest compressed pulse. Note that the shorter wavelength is cut by the second BK7 prism in the precompressor (comparing with Fig. 5). Inset: the intensity profile of the inverse Fourier transform of the measured spectrum.

which may be attributed to some satellite pulses mainly originating from the larger uncompensated negative TOD of the BK7 prism pair (see Table I) [33]. These unpleasant wing shapes of the FRAC cannot be removed by only the prism-pair compressor due to its dispersion-interdependence feature. This fact shows definitely that a programmable SLM in the pulse shaper is quite useful as an independent and accurate dispersion compensator.

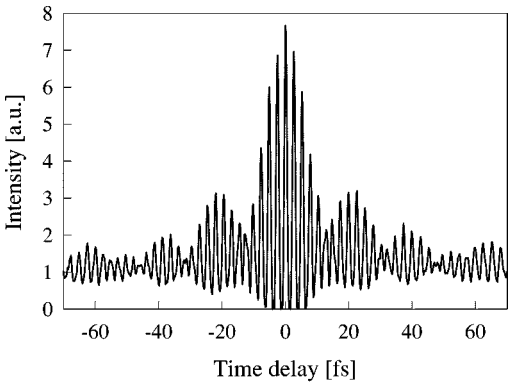

Fig. 8. Measured FRAC of the compressed pulse using a pair of BK7 prisms alone (see text). The large structures on the wings of FRAC attribute to some satellite pulses which mainly originate from the larger uncompensated negative TOD of the BK7 prism-pair.

IV. Discussion

Our Brewster prism-pair-formed pulse shaper with an SLM has about 80% throughout of the energy when the input pulse electric field is parallel to the plane of incidence on the prisms (called p polarization). The losses are mainly introduced by the Al-coated reflective mirrors and the SLM (90% transmission). In our experiment, the SLM that we operate in the pulse shaper is manufactured for s-polarization light (the electric field is orthogonal to the plane of incidence). We have to propagate s-polarization light in the pulse shaper at the expense of high losses from the prisms, resulting in a total output energy behind the pulse shaper of 4$\sim$5 μJ. Fortunately, a commercial SLM for both polarizations (p and s) is presently available (Meadowlark Optics) and, in the end, a low-loss pulse shaper can be realized. In addition, we have observed that the compressed pulse spectral range is limited by the removal of the short wavelengths introduced by the second BK7 prism in the precompressor due to a smaller size of the prism (see Fig. 7). This results in a Fourier transform of the spectrum of 5.6 fs, just a little bit shorter than the compressed pulse. In order to remove the spectral limitation, a larger BK7-glass prism is required and the separation length between prisms can be increased further. Therefore, a larger positive cubic phase must be imparted on the SLM in the pulse shaper. Moreover, the quartic or even higher order phases are not dealt with in our present experiment. This will become more important for further pulse shortening. As we discussed before, the drawback of a prism-pair-formed pulse shaper is the dispersion of the prism material, resulting in a nondispersion-free system. This forces us to increase the separation length of the prisms in the precompressor. Consequently, a larger negative TOD has to be introduced by the SLM. It should be noted that the SLM with a finite pixel number will limit operation to a larger phase controlling because it is hard to apply a rapid varying phase on the edges of the modulator [see Fig. 3(b)]. It can be decreased by using a modulator with $large$ pixel numbers. Theoretical calculations on this effect are underway. In addition, we believe the SLM may ultimately limit pulse compression to the mono-cycle regime due to the fact that the SLM is a discrete system. Phases are controlled in a series of steps instead of a smooth curve. The dead space between pixels will prevent complete phase control of the spectrum and affect the spatial quality of the shaped-pulse because of scattering by the gaps. This effect can be reduced by decreasing the gaps or removed by using a nonpixel phase modulator. As for these points, further investigation is needed.

Despite the drawbacks mentioned above, the programmable technique using a prism-pair-formed pulse shaper still has some advantages compared with the other compensation techniques. First, it has a large bandwidth when using Brewster-angle-cut prisms. Second, it has the ability to provide accurate and independent nonlinear-chirp compensation by an *in situ* phase adjustment during pulse measurements without the realignment of any components. Third, it can be controlled by automatic feedback for adaptive pulse compression [24], [26]. Because of these features, this technique may be applied to compress broad-band pulses recently generated by induced-phase modulation [7], [8], and so the generation of even shorter pulses can be expected in the near future.

V. Conclusion

A TF5 prism-pair-formed pulse shaper capable of programmable chirp compensation has been demonstrated for the first time. A strongly-chirped ultrabroad spectral pulse has been produced by coupling 1-kHz 30-fs 400-μJ pulses into an argon-filled glass capillary fiber at a gas pressure of 2.0 bar. The chirped pulse has been first precompressed by a pair of BK7 prisms with a separation length of 65 cm and then directed to the prism-pair-formed pulse-shaping apparatus with a commercially available 128-pixel SLM, which provides quadratic and cubic phase compensation. When the quadratic and cubic phases have been set to -330 fs^2 and $+2000$ fs^3, respectively, at the wavelength of 760 nm, a 6-fs optical pulse has been generated. This is, to the best of our knowledge, the shortest optical pulse ever compressed using the SLM pulse-shaping technique for chirp compensation. This technique can be applied to monocycle pulse compression due to its unique features.

Acknowledgment

The authors would like to thank N. Karasawa, K. Matsumoto, and S. Nakamura for their help.

References

[1] T. Elsaesser, J. G. Fujimoto, D. A. Wiersma, and W. Zinth, Eds., *Ultrafast Phenomena XI*. Berlin, Germany: Springer-Verlag, 1998.
[2] P. F. Moulton, "Spectroscopic and laser characteristics of Ti : Al_2O_3," *J. Opt. Soc. Amer. B*, vol. 3, pp. 125–132, 1986.
[3] R. R. Alfano and S. L. Shapiro, "Observation of self-phase modulation and small scale filaments in crystals and glasses," *Phys. Rev. Lett.*, vol. 24, pp. 592–594, 1970.
[4] R. R. Alfano, Ed., *The Supercontinuum Lase Source*. New York, NY: Springer-Verlag, 1989.
[5] M. Yamashita, H. Sone, and R. Morita, "Proposal for generation of a coherent pulse ultra-broadened from near-infrared and its monocyclization," *Jpn. J. Appl. Phys.*, vol. 35, pp. L1194–L1197, 1996.
[6] M. Yamashita, H. Sone, R. Morita, and H. Shigekawa, "Generation of monocycle-like optical pulses using induced-phase modulation between two-color femtosecond pulses with carrier phase locking," *IEEE J. Quantum Electron.*, vol. 34, pp. 2145–2149, 1998.

[7] L. Xu, N. Karasawa, N. Nakagawa, R. Morita, H. Shigekawa, and M. Yamashita, "Experimental generation of an ultra-broad spectrum based on induced-phase modulation in a single-mode glass fiber," *Opt. Commun.*, vol. 162, pp. 256–260, 1999.
[8] N. Karasawa, R. Morita, H. Shigekawa, and M. Yamashita, "Generation of intense-ultrabroadband optical pulses by induced-phase modulation in an argon-filled single-mode hollow waveguide," Opt. Lett., to be published.
[9] R. L. Fork, C. H. Cruz, P. C. Becker, and C. V. Shank, "Compression of optical pulses to six femtosecond by using cubic phase compensation," *Opt. Lett.*, vol. 12, pp. 483–485, 1987.
[10] R. Szipöcs, K. Ferencz, Ch. Spielmann, and F. Krausz, "Chirped multilayer coatings for broadband dispersion control in femtosecond lasers," *Opt. Lett.*, vol. 19, pp. 201–203, 1994.
[11] G. Tempea, F. Krausz, Ch. Spielmann, and K. Ferencz, "Dispersion control over 150 THz with chirped dielectric mirrors," *IEEE J. Select. Topics Quantum Electron.*, vol. 4, pp. 193–196, 1998.
[12] F. X. Kärtner, N. Matuschek, T. Schibli, U. Keller, H. A. Haus, C. Heine, R. Morf, V. Scheuer, and T. Tschudi, "Design and fabrication of double-chirped mirrors," *Opt. Lett.*, vol. 22, pp. 831–833, 1997.
[13] N. Matuschek, F. X. Kärtner, and U. Keller, "Theory of double-chirped mirrors," *IEEE J. Select. Topics Quantum Electron.*, vol. 4, pp. 197–208, 1998.
[14] Z. Cheng, G. Tempea, T. Brabec, K. Ferencz, C. Spielman, and F. Krausz, "Generation of intense diffraction-limited white light and 4-fs pulses," in *Ultrafast Phenomena XI*. Berlin, Germany: Springer-Verlag, 1998, pp. 8–10.
[15] A. Baltuška, Z. Wei, M. Pshenichnikov, and D. Wiersma, "Optical pulse compression to 5 fs at a 1-MHz repetition rate," *Opt. Lett.*, vol. 22, pp. 102–104, 1997.
[16] M. Nisoli, S. D. Silverstri, O. Svelto, R. Szipöcs, Ch. Spielmann, S. Sartania, and F. Krausz, "Compression of high-energy laser pulses below 5 fs," *Opt. Lett.*, vol. 22, pp. 522–524, 1997.
[17] A. Shirakawa, I. Sakane, M. Takasaka, and T. Kobayashi, "Sub-5-fs visible pulse generation by pulse-front-matched nonlinear optical parametric amplification," *Appl. Phys. Lett.*, vol. 74, pp. 2268–2270, 1999.
[18] U. Morgner, F. X. Kärtner, S. H. Cho, Y. Chen, H. A. Haus, J. G. Fujimoto, and E. P. Ippen, "Sub-two-cycle pulses from a Kerr-lens mode-locked Ti : sapphire laser," *Opt. Lett.*, vol. 24, pp. 511–513, 1999.
[19] D. H. Sutter, G. Steinmeyer, L. Gallmann, N. Matuschek, F. Morier-Genoud, and U. Keller, "Semiconductor saturable-absorber mirror-assisted Kerr-lens mode-locked Ti : sapphire laser producing pulses in the two-cycle regime," *Opt. Lett.*, vol. 24, pp. 631–633, 1999.
[20] A. M. Weiner, D. E. Leaird, J. S. Patel, and J. R. Wullert, "Programmable shaping of femtosecond optical pulse by use of 128-element liquid crystal phase modulator," *IEEE J. Quantum Electron.*, vol. 28, pp. 908–920, 1992.
[21] A. Efimov, C. Schaffer, and D. H. Reitze, "Programmable shaping of ultrabroad-bandwidth pulses from a Ti : sapphire laser," *J. Opt. Soc. Amer. B*, vol. 12, pp. 1968–1980, 1995.
[22] M. A Dugan, J. X. Tull, and W. W. Warren, "High-resolution acousto-optic shaping of unamplified and amplified laser pulses," *J. Opt. Soc. Amer. B*, vol. 14, pp. 2348–2358, 1997.
[23] E. Zeek, K. Maginnis, S. Backus, U. Russek, M. Murnane, G. Mourou, and H. Kapteyn, "Pulse compression by use of deformable mirrors," *Opt. Lett.*, vol. 24, pp. 493–495, 1999.
[24] D. Yelin, D. Meshulach, and Y. Silberberg, "Adaptive femtosecond pulse compression," *Opt. Lett.*, vol. 22, pp. 1793–1795, 1997.
[25] A. Efimov and D. H. Reitze, "Programmable dispersion compensation and pulse shaping in a 26-fs chirped-pulse amplifier," *Opt. Lett.*, vol. 23, pp. 1612–1614, 1998.
[26] T. Brixner, M. Strehle, and G. Gerber, "Feedback-controlled optimization of amplified femtosecond laser pulses," *Appl. Phys. B*, vol. 68, pp. 281–284, 1999.
[27] C.-C. Chang, H. P. Sardesai, and A. M. Weiner, "Dispersion-free fiber transmission for femtosecond pulses by use of a dispersion-compensating fiber and a programmable pulse shaper," *Opt. Lett.*, vol. 23, pp. 283–285, 1998.
[28] F. A. Jenkins and H. E. White, *Fundamentals of Optics*, third ed. New York, NY: McGraw-Hill, 1957.
[29] *AVESTA Company of Russia*
[30] J.-C. Diels and W. Rudolph, *Ultrashort Laser Pulse Phenomena: Fundamentals, Techniques, and Applications on a Femtosecond Time Scale*. New York, NY: Academic, 1995.
[31] M. Bass, *Handbook of Optics*. New York, NY: McGraw-Hill, 1995.
[32] J.-C. Diels, J. J. Fontaine, I. C. McMichael, and F. Simoni, "Control and measurement of ultrashort pulse shapes (in amplitude and phase) with femtosecond accuracy," *Appl. Opt.*, vol. 24, pp. 1270–1282, 1985.
[33] F. Krausz, M. Fermann, T. Brabec, P. Curley, M. Hofer, M. Ober, Ch. Spielmann, E. Wintner, and A. Schmidt, "Femtosecond solid-state lasers," *IEEE J. Quantum Electron.*, vol. 28, pp. 2097–2122, 1992.

Lin Xu (M'00) received the B.S. degree in optoelectronics from Tsinghua University, China, in 1988, the M.Sc. degree in laser physics from Xian Institute of Optics & Precision Mechanics, the Chinese Academy of Science, in 1992, and the Ph.D. degree in laser physics from Vienna University of Technology in 1998.

He joined the Department of Applied Physics, Hokkaido University, Sapporo, Japan, as a Researcher from February 1998 to Decemeber 1999, supported by Japan Science and Technology Corporation (JST). Since January 2000, he has been with the School of Physics, Georgia Institute of Technology, Atlanta, as a Postdoctoral Fellow. His researcher interests focus on femtosecond lasers, pulse measurement, nonlinear optics, and ultrafast applications. He is the author or co-author of more than 40 journal or conference contributions in the field of ultrafast optics.

N. Nakagawa, photograph and biography not available at the time of publication.

R. Morita, photograph and biography not available at the time of publication.

H. Shigekawa, photograph and biography not available at the time of publication.

M. Yamashita, photograph and biography not available at the time of publication.